Astron. Astrophys. 354, 657–666 (2000)

ASTRONOMY AND ASTROPHYSICS

A dust envelope modelling of the Egg Nebula

B. Lopez[1] **and J.-M. Perrin**[2]

[1] Observatoire de la Côte d'Azur, Département Fresnel UMR 6528, B.P. 4229, 06034 Nice Cedex 4, France
[2] Observatoire de Haute Provence, UPR A9049, 04870 Saint Michel l'Observatoire, France

Received 7 July 1999 / Accepted 29 September 1999

Abstract. Radiative transfer modelling of the dust envelope of the post-AGB (post-Asymptotic Giant Branch) object called the Egg nebula is proposed in non-spherical geometry. The present work follows a previous study by Yusef-Zadeh et al. (1984) in which the dust density law smoothly decreases with latitude above and below the midplane of a disk shaped envelope.

The model we present reproduces the broad band spectrum and the bipolar structures of the Egg nebula as observed at various wavelengths from visible to mid-infrared. Dust particles as large as 8 μm in radius are required in the model to fit the observations. We estimate the mass of the dust envelope to be about $4.4 \times 10^{-2} M_{\odot}$ assuming a distance of 1000 pc. According to a mass ratio of gas to dust of 158 (Knapp 1986), the total mass of the envelope of the Egg Nebula is estimated to be 7.0 $M_{\odot}$. We compare our results to those of a recently published paper (Skinner et al. 1997) and compare our model geometry to a sketch proposed by Sahai et al. (1998b).

Key words: radiative transfer – stars: circumstellar matter – stars: AGB and post-AGB – ISM: individual objects:

1. Introduction

1.1. General aspects of the Egg Nebula

The Egg Nebula (CRL 2688) is a very beautiful bipolar nebula which belongs to the post-AGB phase of stellar evolution (a phase of the evolution of low and intermediate mass stars). The size of the nebula at the visible wavelength is larger than 70 arcsec (Ney et al. 1975). The nebula, composed of gas and dust, is the result of the mass loss history of the star, which traces the last 13000 years (assuming d = 1 kpc, Sahai et al. 1998a).

The shape of the bipolar nebula (Ney et al. 1975) is linked to a disk-like envelope geometry. This disk where the material is concentrated is nearly seen edge-on. At large spatial scale, the structure of the Egg Nebula is remarkably symmetric from visible to mid-infrared wavelengths and displays spike-like features also called searchlight beams (Sahai et al. 1998a). At shorter spatial scales, bright arcs, which correspond to fluctuations in the dust density, are observed. These fluctuations may trace temporal variations of the mass loss toward the interstellar medium (Harpaz et al. 1997; Sahai et al. 1998a and 1998b).

The Egg Nebula is a post-AGB carbon star (Zuckerman et al. 1976), its molecular envelope emission is very similar to the one of the carbon star IRC+10216.

1.2. Our goal

The high optical depth of the disk-like envelope that is seen edge-on and the presence of large dust particles which scatter efficiently the light up to mid-infrared wavelengths together contribute to the occurrence of the two well detached bright lobes of the nebula.

For reproducing the appearance of the nebula at visible wavelengths through modelling, Yusef-Zadeh et al. (1984) have analysed the role played by several model parameters: the geometry of the envelope, the optical depth of the envelope, the albedo and the scattering diagram of the dust particles.

In our present study, we extend the Yusef-Zadeh et al. (1984) investigation in order to establish a model of the Egg Nebula coherent with a wider range of observational constraints. Any image up to infrared wavelengths but also the spectral energy distribution of the object which contains dust thermal radiation contributions has been modelled here. A wider range of physical parameters can thus be estimated. To achieve this goal, the radiative transfer code we use, simulates the radiative transfer and also computes the radiative equilibrium of the dust grains (i.e. the temperature of the grains).

We compare the results of our model to a recently published similar paper (Skinner et al. 1997). While processing our Egg nebula models, we were not in touch with Christopher Skinner and his collaborators and did not know about their work. This is an interesting condition since the present comparison is made between two truly independent modellings.

The dust envelope geometry we use (a smoothly variable dust distribution) is compared to a sketch displayed in the paper of Sahai et al. (1998b, Fig. 5).

2. The modelling of the stellar dusty environment

2.1. Our approach for the dust envelope geometry

They are at least two possible approaches:

Send offprint requests to: Bruno Lopez (lopez@obs-nice.fr)

- one is to consider that the disk forming the nebula has a limited extent compared to the size of the extended lobes. For example the disk of dust may have the shape of a optically thick torus surrounded by regions of lower dust density. The external size of such a torus may be smaller than the overall size of the nebula. According to this sketch, the center of the Egg nebula may contain a thick cocoon of dust as proposed in Fig. 5 of Sahai et al. (1998b).
- alternatively, Morris (1981) has shown that the dusty envelopes like the one of the Egg Nebula may be represented by a dust density law smoothly decreasing with latitude above (and below) the midplane. In this geometry, the radial extent of the envelope is identical at all latitudes. The geometrical model proposed by Morris (1981) has been successfully exploited by Yusef-Zadeh et al. (1984) who studied the latitude distribution of dust particles for the Red Rectangle, the Egg Nebula and M1-92.

We think that in the present state of what we know on the Egg Nebula, there is no way to discriminate between the two possibilities. No thick torus of dust has been yet detected from observations and hence no serious constraints impose the use of a model constituted by a torus surrounding the star. Although not more realistic, we use the Morris suggested geometry mostly because it is complex enough and well suited to explain the large spatial scale morphology of the envelope. Smaller spatial scale features such as the "rings" or "multiple arcs" (Sahai et al. 1998a and 1998b), clearly visible in HST images are not modelled in the present paper.

2.2. The simulation / radiative transfer code

The radiative transfer and radiative equilibrium is solved by a numerical simulation which is based on a Monte Carlo method. This method was often used in the case of spherical geometry (see for example Lefèvre et al. 1982) and was applied to axisymmetric dust nebulae (Lopez et al. 1995).

The numerical simulation aims at solving the problem of multiscattering into a dust envelope that may be optically thick for certain wavelengths and at computing the temperature of the grains.

The spatial dust grain distribution is an axisymmetric function $D(r, \delta)$, δ being the latitude angle from the plane of the disk and r the radial distance from the center of the star given in photospheric radius units. The function $D(r, \delta)$ is bounded by inner and outer limits denoted R_{int} and R_{out} respectively. The grains are assumed to be of spherical shape (radius a) and composed of homogeneous, isotropic, linear materials. The Mie's theory can be used to calculate the extinction (C_{ext}), the scattering (C_{sca}) and the absorption (C_{abs}) cross sections and is used to describe the angular dependence of the scattered intensity.

As the size of the dust particles could be large (compared to the wavelength) as well as the values of the complex index of refraction, the Mie's algorithm of Wiscombe is used (Wiscombe, 1980). This algorithm allows us to avoid instabilities using the Lentz method (i.e. generating, if necessary, the components of one normal mode independently of lower or upper order modes).

According to the Monte Carlo method, stellar radiations and the thermal emission from dust particles are generated by a set of radiation trajectories. Thirty wavelengths are used to represent the emergent spectrum from the star and the spectra of dust particles.

At the beginning of the algorithm, radiation is first emitted by the star which is represented by a sphere. The direction of initial propagation of one ray is chosen randomly isotropically from one point of the star. The location of the interaction of the radiation with a grain of the dusty envelope is chosen randomly. The density probability of the random process is proportional to exp(-τ), where τ is the optical depth along the direction of propagation.

Along a radial direction, the spatial dust grain distribution function is related to the optical depth τ_{ext} by:

$$\tau_{ext}(a, \lambda, \delta) = \int_{R_{int}}^{R_{out}} D(r, \delta) C_{ext}(a, \lambda) dr \quad (1)$$

For each interaction, a fraction of the radiation leaves the envelope, a fraction is absorbed and a fraction is scattered. The direction of scattering is randomly choosen, weighted using $i(\theta)$ (which describes the scattering diagram). The scattered fraction of the radiation continues then to propagate in the three dimensional dusty medium. Several interactions with dust grains will successively occur, ten scatterings were allowed here. After this multiple scattering, new radiations are then generated from the star as well as later in the process from thermally emitting dust particles.

The star is assumed to radiate as a blackbody and is characterized by its effective temperature $T_\star$. This is a rough approximation but uncertainties about the true radiative properties of the central star do not justify a better model. In the present simulation the dust shell is sampled in about 400 tori in each of which the grain temperature is constant for axisymmetry reasons. Radiative exchanges between the star and tori and between each torus and other tori constrain the radiative equilibrium relation. Assuming negligeable sublimation, this relation which equates in each torus the total amount of absorbed energy to the total amount of emitted energy, provides the temperature of the dust.

The brightness distribution of the object (as a function of wavelength and inclination angle of the nebula) as well as its broad band spectrum (depending also on inclination angle of the nebula) are obtained for a given set of parameters characterizing the model. A solution for the parameters is searched for empirically until the results of the simulation reproduce the existing measurements.

2.3. The results

First attemps of modelling show that the observational constraints considered, i.e. the broad band spectrum and the morphology of the nebula at visible and near infrared wavelengths, cannot be reproduced with a unique size of dust particles and without considering large dust grain size (at least with a radius of $5\mu m$). The part of the spectrum containing the visible wavelengths up to about 3 μm of wavelength can be fitted only if a

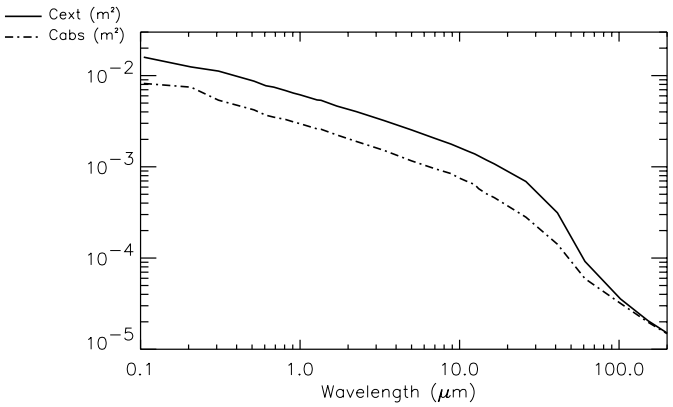

Fig. 1. Mean optical properties for the size distribution of amorphous carbon grains used in our model.

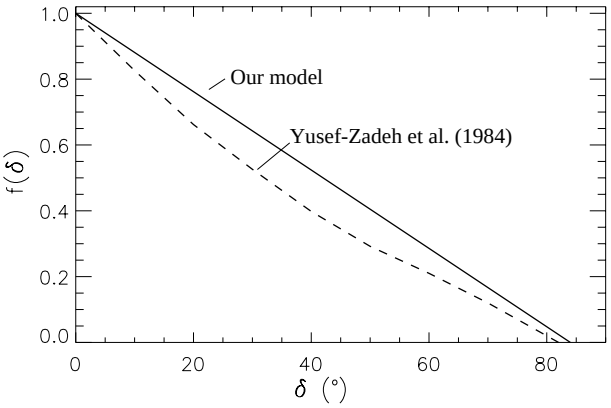

Fig. 2. The density laws.

"grey-like" extinction of the stellar radiation is produced in the model, large grains are required for this. Moreover, the bipolar aspect of the Egg nebula which holds at least up to 5 μm of wavelength are produced mostly due to the contribution of scattering by dust, an efficient scattering is obtained when the dust size is comparable to the wavelength.

A distribution of grain dimensions is therefore considered. The grain size distribution used in our new model is:

$$dn \propto a^{-\beta} da \tag{2}$$

Ideally, the computation of radiative transfer by a Monte Carlo method would require a random choice (weighted using $a^{-\beta}$) of the size of the grain which interacts with the radiation field. However, for practical reasons the optical grain properties are averaged over the different sizes and hence lead to a kind of hybrid grain (see Fig. 1 which displays the values of C_{abs} and C_{ext} versus the wavelength). While the equilibrium temperatures of grains of different sizes located at the same distance from the star are expected to differ, the use of a hybrid grain leads to a mean value for the temperature.

Optical properties are averaged according to the following relations,

$$\langle C_{abs}(a,\lambda)\rangle = \int_{a_{min}}^{a_{max}} C_{abs}(a,\lambda) a^{-\beta} da \; / \; \int_{a_{min}}^{a_{max}} a^{-\beta} da \tag{3}$$

and

$$\langle C_{sca}(a,\lambda)\rangle = \int_{a_{min}}^{a_{max}} C_{sca}(a,\lambda) a^{-\beta} da \; / \; \int_{a_{min}}^{a_{max}} a^{-\beta} da \tag{4}$$

where C_{abs} and C_{sca} are the optical cross sections for absorption and scattering. The mean phase function $\langle i(\theta)\rangle$ is given by,

$$\langle i(\theta,a,\lambda)\rangle = \int_{a_{min}}^{a_{max}} i(\theta,a,\lambda) a^{-\beta} da \; / \; \int_{a_{min}}^{a_{max}} a^{-\beta} da \tag{5}$$

Many model parameters have been tried. The best results have been obtained with the latitude functions, $f(\delta)$, displayed in Fig. 2. The following parameters reproduce reasonably well the observations (see also Table 1):

- $T_{eff} = 7000$ K
- the angular radius of the star $\alpha_* = 0.56 \times 10^{-3}$ arcsec (consistent with the amount of the received bolometric flux)
- $R_{int} = 600 R_\star$; $R_{ext} = 30000 R_\star$
- $D(r,\delta) \propto f(\delta) \times r^{-2}$.
- Dust particles are supposed to be composed of amorphous carbon.
- $\tau_{ext}(\lambda = 1\mu\text{m}, \delta = 0^\text{o}) = 26$ in the plane of the disk.
- 0.02μm$< a < 8\mu$m with a size distribution of $a^{-3.5}$.

With this set of parameters:

- a good fit to the emergent spectrum (see Fig. 3) is obtained from 0.10 to about 200 μm (200 μm being the maximum wavelength for which the radiative transfer is here simulated).
- The images simulated for 0.55μm of wavelength up to 18μm are shown in Figs. 4, 5, 6, 7, 8, 9, 10 and 11. Different inclinations of the plane of the disk with respect to the line of sight are considered. The Egg Nebula morphology holds for an inclination angle less that 10^o. The shapes of the near-IR simulations are consistent with the Sahai et al. (1998b) and Latter et al. (1993) observations.
- As for the models of Yusef-Zadeh et al. (1984), the spikes of the nebula clearly seen in the images at visible wavelengths of the Egg Nebula can be grossly reproduced (see the grey scaled Fig. 6 which gives a better display of the spikes than a contour plot).

3. Discussion

3.1. What do we learn from the Egg Nebula?

The model detailed above is coherent with a large body of observational data. It allows us to derive or rather, more modestly,

Table 1. Egg Nebula model parameters.

Model parameters

T_{eff}	ang. radius α_*	R_{int}	R_{ext}	a grains	D(r, δ)	$\tau_{ext}(\lambda=1\mu m, \theta=0^o)$
7000 K	0.56 mas	$600R_*$	$30000R_*$	from 0.02 to 8.0 μm	prop. to $f(\delta).r^{-2}$	26

d	R_*	T of the hottest dust	M_{shell}
1000 pc	R_{sun}	about 330 K	$4.4\ 10^{-2}$ solar masses of dust

Quantities deduced from the model

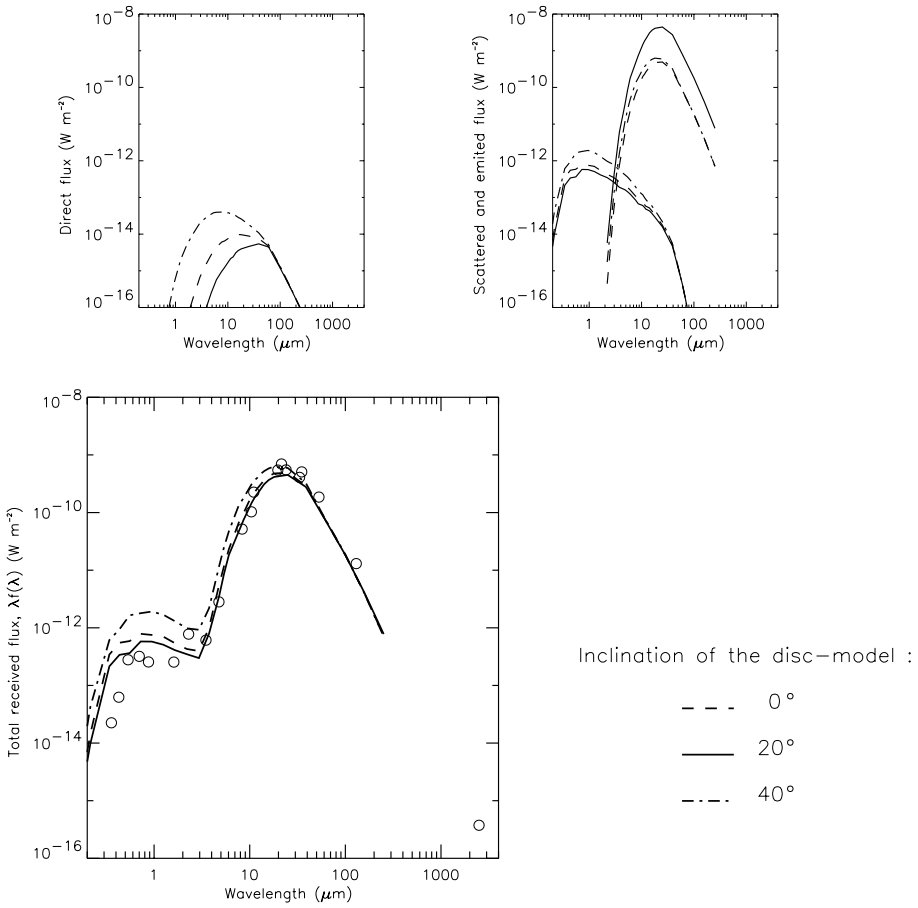

Fig. 3. The broad band spectrum of the Egg Nebula compared to the model fit for different view angles of the disk. The photometric data are from a compilation of Ney et al. (1975) and Skinner et al. (1997).

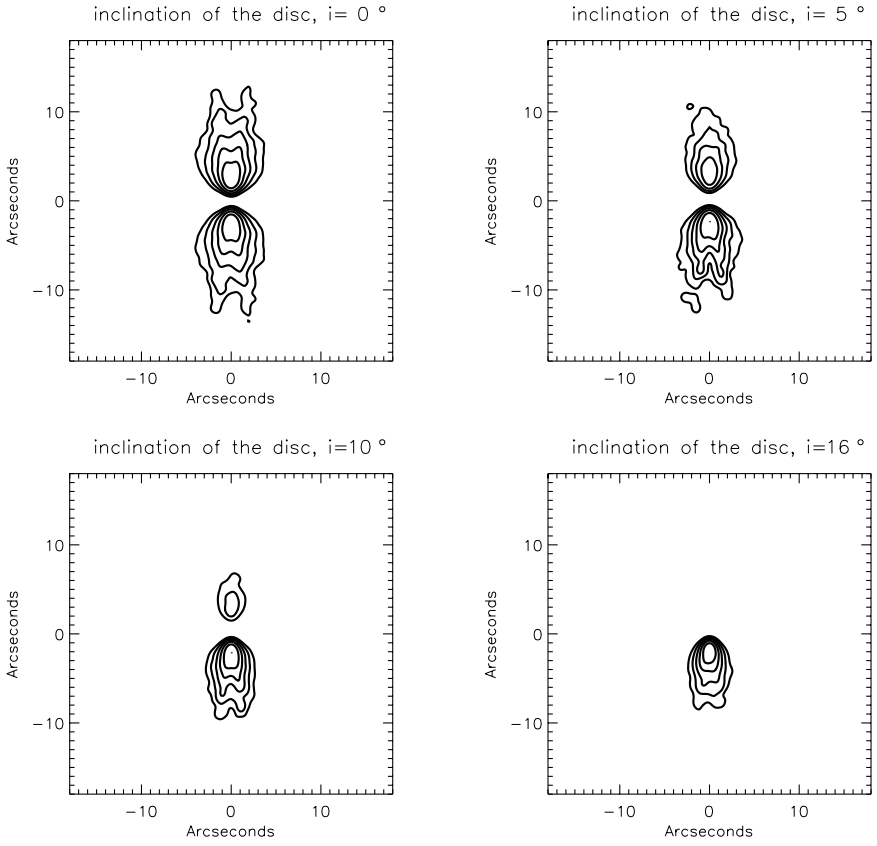

Fig. 4. Contour plot of the images simulated at 0.55 μm for different view angles. Each image is convolved by a Gaussian with σ=0.4 arcsec. The ratio between two successive contour levels is $10^{0.2}$.

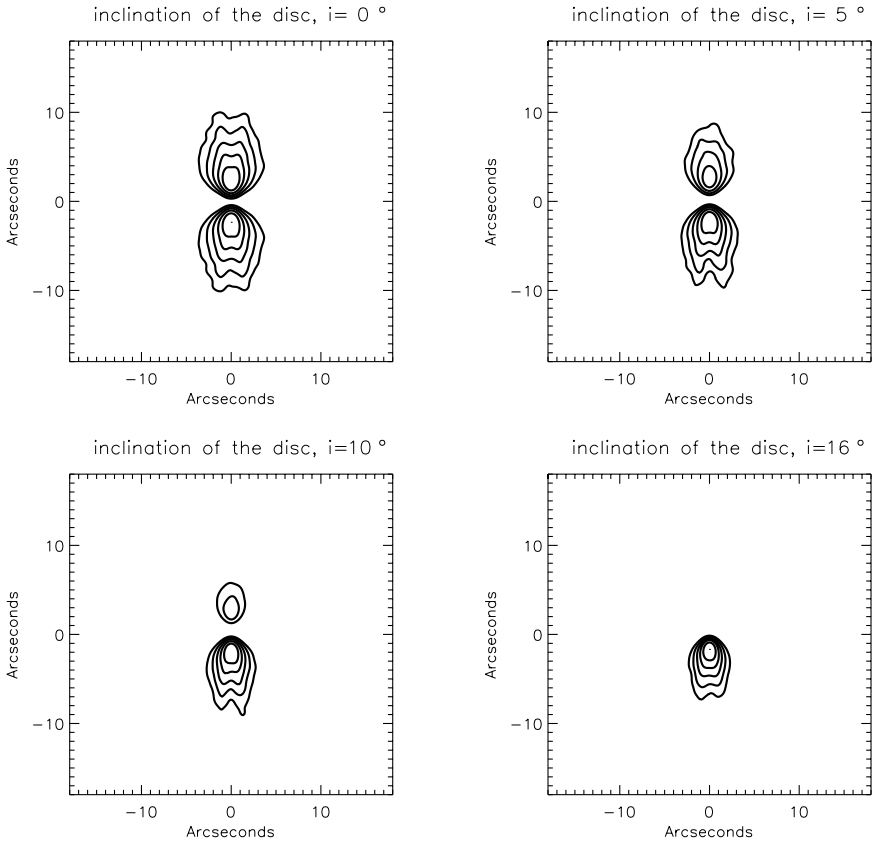

Fig. 5. Contour plot of the images simulated at 0.72 μm for different view angles. Each image is convolved by a Gaussian with σ=0.4 arcsec. The ratio between two successive contour levels is $10^{0.2}$.

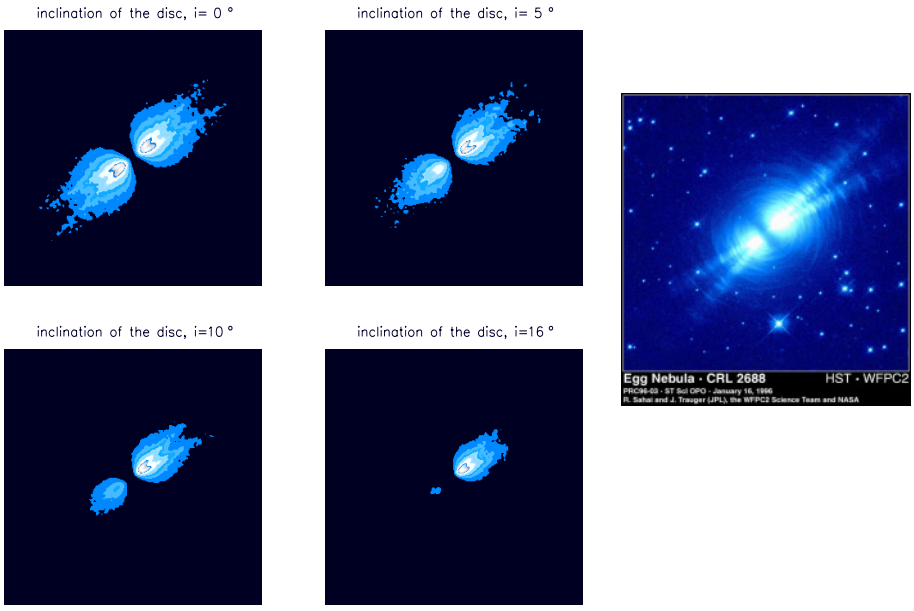

Fig. 6. Grey scale plot of the images simulated at 0.72 μm for different view angles compared to the image taken by Sahai and Trauger with the HST. Courtesy of the HST WWW image gallery, reproduced with the permission of the authors.

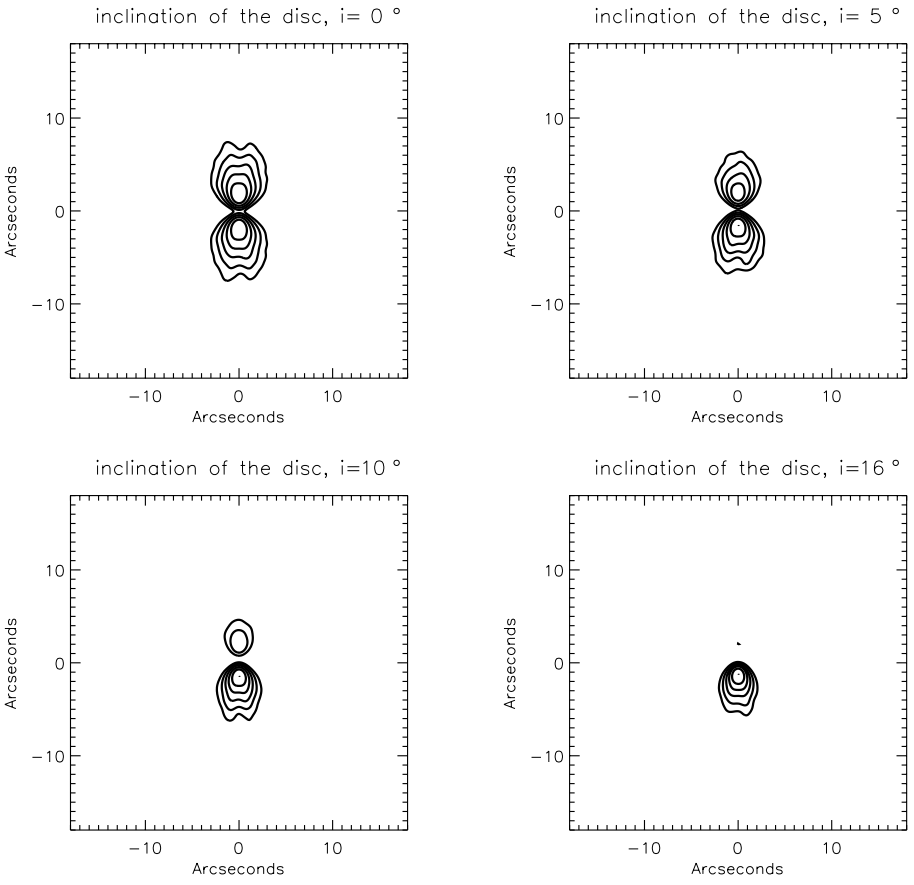

Fig. 7. Contour plot of the images simulated at 1.25 μm for different view angles. Each image is convolved by a Gaussian with σ=0.4 arcsec. The ratio between two successive contour levels is $10^{0.2}$.

to estimate, some astrophysical quantities that are discussed below.

The temperature of the hottest dust grains (located near the star) is about 300K. Presently this value for the temperature is obtained supposing that a thermal equilibrium is reached. Moreover, the absorbed energy being supposed to be balanced by the radiated energy, means that the energy removed by sublimation is neglected. Is this hypothesis valid? Our model uses grains of amorphous carbon (Rouleau and Martin 1991). This material is a carbon black obtained by striking an arc between pure amorphous carbon electrodes in a controlled argon atmosphere (see for example Bussoletti et al. 1987). It is made of small graphitic

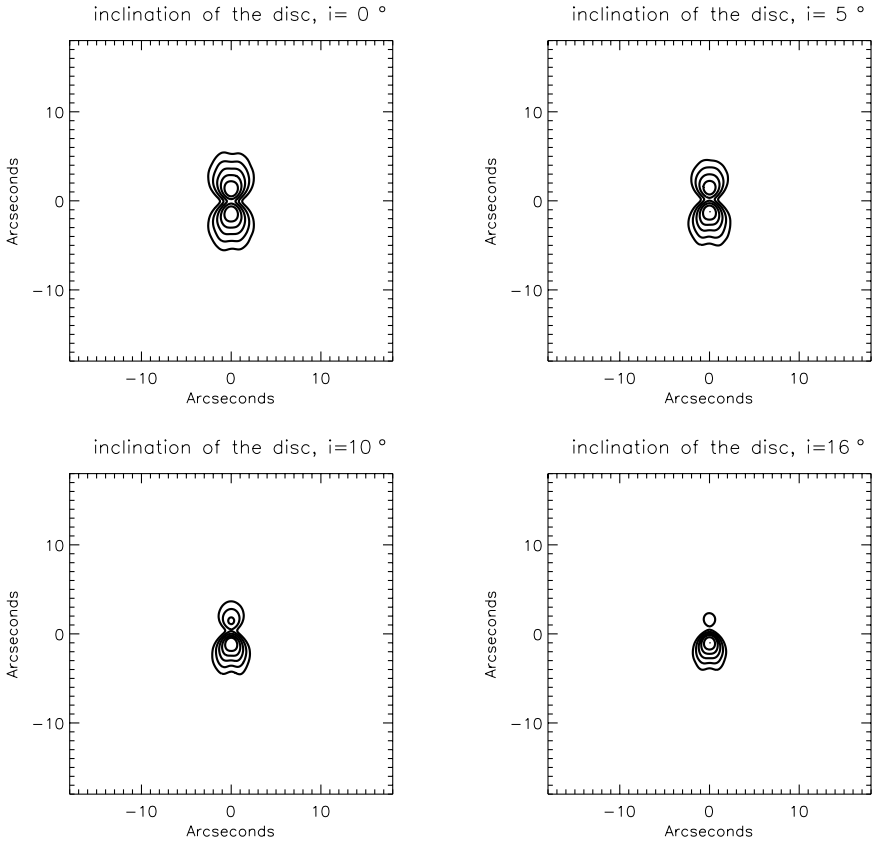

Fig. 8. Contour plot of the images simulated at 2.2 μm for different view angles. Each image is convolved by a Gaussian with σ=0.4 arcsec. The ratio between two successive contour levels is $10^{0.2}$.

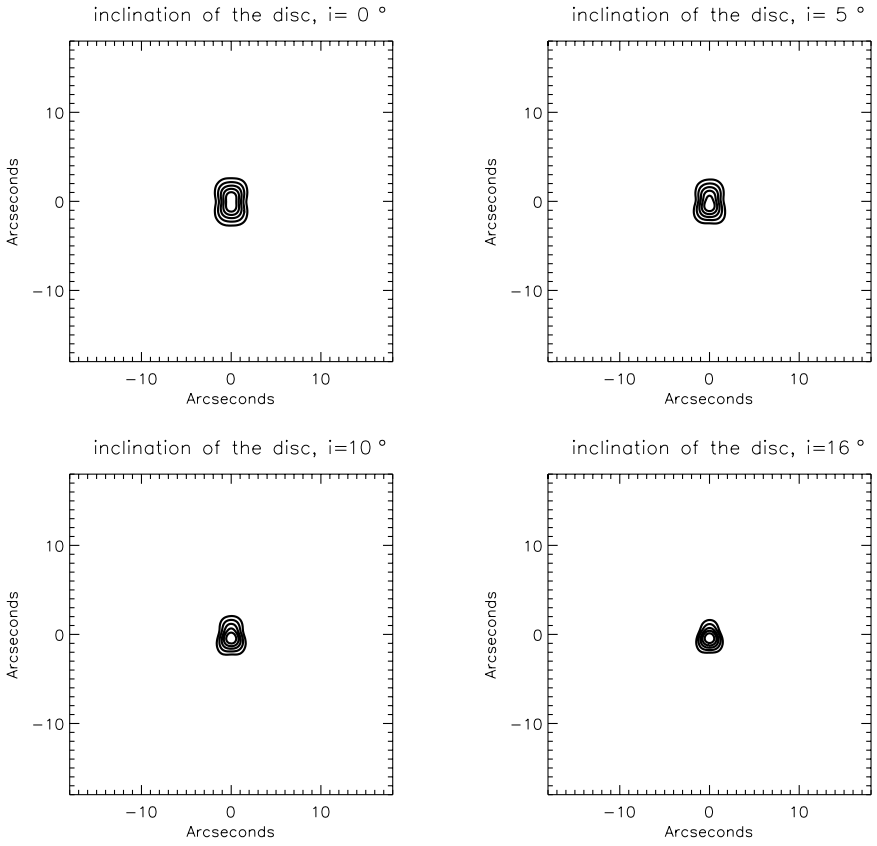

Fig. 9. Contour plot of the images simulated at 5.39 μm for different view angles. Each image is convolved by a Gaussian with σ=0.4 arcsec. The ratio between two successive contour levels is $10^{0.2}$.

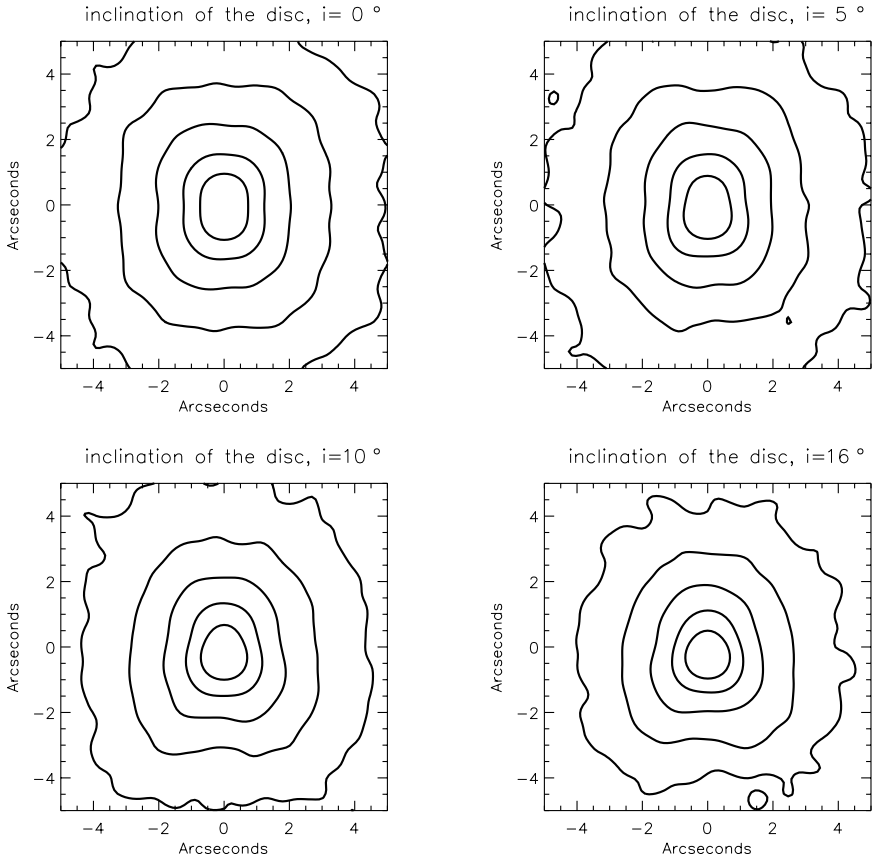

Fig. 10. Contour plot of the images simulated at 8.62 μm for different view angles. Each image is convolved by a Gaussian with σ=0.3 arcsec. The ratio between two successive contour levels is $10^{0.5}$.

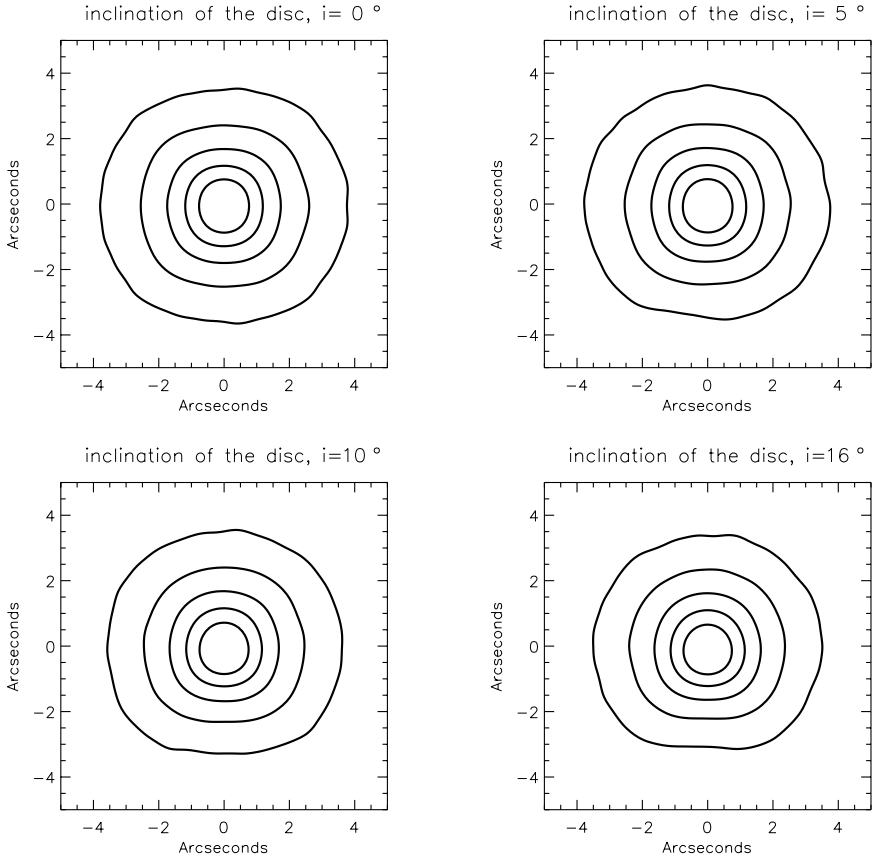

Fig. 11. Contour plot of the images simulated at 18.00 μm for different view angles. Each image is convolved by a Gaussian with σ=0.3 arcsec. The ratio between two successive contour levels is $10^{0.5}$.

bricks linked with glassy carbon-like structures (Papoular et al. 1996). Phase diagrams show that such carbonaceous components need to sublimate at 300K and at larger pressures than those encountered in the envelope of the Egg Nebula. Thus our hypothesis is valid.

According to our model, the number density of dust particles in the equatorial plane and at the inner limit of the disk is,

$$D(r = 600R_\star, \delta = 0^o) = 3.72 \times 10^5 \times d^{-1} \text{ grains.m}^{-3} \quad (6)$$

Where d is the distance of the source. This distance is uncertain and estimated to be about 1 kpc by Crampton et al. (1975) while Cohen and Kuhi (1977) estimate a distance of 1.5 kpc. If we take $\rho = 2.2\ 10^3$kg m^{-3} for the mass density of the dust grains, the mass of grains per unit volume at the inner limit of the disk is $2.36 \times 10^{-12} \times d^{-1}$ kg.m^{-3}

The mass of grains contained in the whole envelope is:

$$M_{grains\ in\ the\ shell} = 4.4 \times 10^{-8} \times d^2\ \mathrm{M}_\odot \quad (7)$$

With d = 1000 pc, $M_{grains\ in\ the\ shell}$ is about $4.4 \times 10^{-2}\mathrm{M}_\odot$. In our model, R_{ext} = 30000 R_* corresponds on the sky to nearly 17 arcsec. This is approximately the size of the angular extent of the reflection nebulosity. If some dust located at larger distance and not detected in the present images exists (dust related to the past AGB wind) then the total dust mass value given above is a minimum. Assuming that the mass ratio of gas to dust is 158 ± 13 (Knapp 1986), the total mass of the envelope is estimated to be $7.0\ \mathrm{M}_\odot$. However, this mass presented here as a minimum has to be taken with care, because the mass loss is considered here, for practical reasons of our model ($D(r, \delta) \propto r^{-2}$), constant with time assuming a constant velocity outflow, although Yamamura et al. (1995) and Sahai et al. (1998b) show that the mass loss rate was lower in the past. A lower mass loss rate episode, in the history of the nebula, may change our total mass envelope estimate. Although the contour plots we obtain are close to the one displayed in the observed images, this pushes us to improve the model by comparing more accurately the radial brightness profiles of the nebula to what will be produced by different dust density laws. This important improvement is not considered in the present paper because it was already a hard and long task to reproduce the gross characteristics of the nebula.

Grain radii up to 5μm in size should exist in the nebula. The presence of such large grains is needed in the model in order to reproduce the observations: the part of the spectrum containing the visible wavelengths up to about 3 μm of wavelength can be fitted only if a "grey-like" extinction of the stellar radiation is produced in the model, and the bipolar shape of the Egg Nebula requires an efficient scattering by dust to be reproduced, at least up to 5 μm of wavelength. Skinner at al. (1997) have proposed some models which also involve a concentration of dust in an equatorial plane but with different geometries/orientations to what is employed in the "standard models". In the Skinner et al's models which demonstrate the gross morphology of the nebula, a unique grain size of 0.1μm was used. This unique grain size value considered by these authors can be compared to the root mean square of the grain radius of the size distribution used in our model, i.e. $2.1 \times 10^{-2}\mu$m.

Assuming a density law decrease represented by a power law with the radial distance (independently of the latitude angle δ), may be far from reality, as said in paragraph 2.1.. An alternative sketch with a central "cocoon" has been proposed by Sahai et al. (1998b Fig. 5). This is compatible with the conclusion of Jura et al. (1995) on the existence of a long-lived disk for another bipolar post-AGB nebula, the Red Rectangle.

The smooth density law we use in our model is able to reproduce the spikes or searchlight beams of the nebula. This was shown already by Yusef-Zadeh et al. (1984); the spikes may be produced by a cutoff of the density law (here for $\delta = 82^\circ$). We feel in fact that the two hollows presented in Fig. 5 of Sahai et al. (1998b) is a sketch possibly closer to reality. This is because direct evidence of polar jets that propagate and generate a kind of bicone-like feature in the polar lobe of the Frosty Leo nebula (Roddier et al. 1995), reinforces the searchlight beam sketch. These probably high speed and density law jets may result from the presence of a companion star that affects the mass loss geometry in a way described by Morris (1987).

From an evolutionary point of view, the Egg Nebula is more evolved than the "best studied carbon star in the universe (by humans)", IRC+10216 (citation from Groenewegen 1997). The molecular envelope emissions compare well (Zuckerman et al. 1976). The mass of the envelope of the Egg nebula we derive from our model is 7.0 $M_\odot$; this result that we consider as a rough estimate, suggests that the initial mass of the star was fairly large and probably at the limit of what is expected for an intermediate mass star (i.e. $8M_\odot$). The envelope mass determined by Skinner et al. is a factor of 2 lower, between 2.9 and 3.6 $M_\odot$, and implies that the initial mass of the star was larger than 4 $M_\odot$. By comparison the initial mass of the progenitor star of IRC+10216 is expected to be between 3.0 and 5.0 $M_\odot$ (Groenewegen 1997, Guélin et al. 1995). One question for the Egg Nebula can be addressed: if the estimates of several solar masses for the total mass of the envelope are valid, then is this consistent with the dynamical age of 13000 years of the envelope?

There are several new steps that can be taken to complete this study. It is relevant to consider a disk limited in extension, like a cocoon, in our model and see what may change in the model parameter determinations. We also wish to study the variability of the mass loss towards the interstellar medium during the last few thousand years, the history of the mass loss variability can be constrained, through modelling, by the concentric "rings" observed in the nebula.

The use of the 10μm long baseline interferometers like the VLTI for the study of the heart of the Egg Nebula is envisaged.

Acknowledgements. A thought goes to Chris Skinner. We met at Baltimore and discussed doing some independent modelling of the carbon star IRC+10216. Our goal was to make more reliable the use of non-spherical (axisymmetric) modelling. Life ends sometimes suddenly, I wish to meet Chris somewhere else and I wish that the above comparison between our two independant models of the Egg Nebula is welcome to his memory. I thank Raghvendra Sahai for allowing us to display the HST image of the Egg Nebula and Jean-Marc Petit for help in the software development.

References

Bussoletti E., Cohugeli L., Borghesi A., Orofino U., 1987, A&AS 70, 257
Cohen M., Kuhi L.V., 1977, ApJ 213, 79
Crampton D., Cowley A., Humphreys R., 1975, ApJ 198, L135
Groenewegen M.A.T., 1997, AetA 317, 503
Guélin M., Forestini M., Valison P., et al., 1995, A&A 297, 183
Harpaz A., Rappaport S., Soker N., 1997, ApJ 487, 809
Jura M., Balm S.P., Kahane C., 1995, ApJ 453, 721
Knapp G.R., 1986, ApJ 311, 731
Latter W.B., Hora J.L., Kelly D.M., Deutsch L.K., Maloney P.R., 1993, AJ 106, 260
Lefèvre J., Bergeat J., Daniel J.Y., 1982, A&A 114, 341
Lopez B., Mékarnia D., Lefèvre J., 1995, A&A 296, 752
Morris M., 1981, ApJ 249, 572
Morris M., 1987, PASP 99, 1115
Ney E.P., Merrill K.M., Becklin E.E., Neugebauer G., Wynn-Williams C.G., 1975, ApJ 198, L129
Papoular R., Conard J., Guillois O., et al., 1996, A&A 315, 222
Roddier F., Roddier C., Graves M.E., Northcott M.J., 1995, ApJ 443, 249
Rouleau F., Martin P.G., 1991, ApJ 377, 526
Sahai R., Hines D.C., Kastner J.H., et al., 1998a, ApJ 492, L163
Sahai R., Trauger J.T., Watson A.M., et al., 1998b, ApJ 493, 301
Skinner C.J., Meixner M., Barlow M.J., et al., 1997, A&A 328, 290
Wiscombe W.J., 1980, Applied Optics 19, 1505
Yamamura I., Onaka T., Kamijo F., Deguchi S., Ukita N., 1995, ApJ 439, L13
Yusef-Zadeh F., Morris M., White R., 1984, ApJ 278, 186
Zuckerman B., Gilra D.P., Turner B.E., Morris M., Palmer P., 1976, ApJ 205, L15